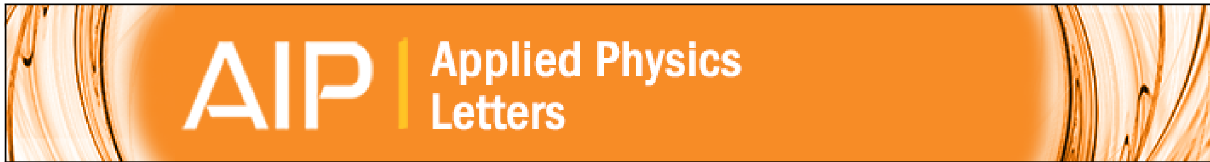

Metal transport and loss in ultrathin hafnium aluminate films on silicon studied by low, medium, and high energy ion beam analyses

L. Miotti, C. Driemeier, F. Tatsch, C. Radtke, and I. J. R. Baumvol

Citation: Applied Physics Letters **89**, 012904 (2006); doi: 10.1063/1.2219150
View online: http://dx.doi.org/10.1063/1.2219150
View Table of Contents: http://scitation.aip.org/content/aip/journal/apl/89/1?ver=pdfcov
Published by the AIP Publishing

Articles you may be interested in
A charge transport study in diamond, surface passivated by high-k dielectric oxides
Appl. Phys. Lett. **105**, 202102 (2014); 10.1063/1.4901961

High resolution medium energy ion scattering analysis for the quantitative depth profiling of ultrathin high- k layers
J. Vac. Sci. Technol. B **28**, C1C65 (2010); 10.1116/1.3248264

Atomic transport and integrity of Al_2O_3 (2.0 nm)∕HfO_2 (2.5 nm) gate stacks on Si
Appl. Phys. Lett. **90**, 052913 (2007); 10.1063/1.2437708

Characteristics of remote plasma atomic layer-deposited HfO_2 films on O_2 and N_2 plasma-pretreated Si substrates
J. Vac. Sci. Technol. A **24**, 678 (2006); 10.1116/1.2194029

Compositional stability of hafnium aluminates thin films deposited on Si by atomic layer deposition
Appl. Phys. Lett. **86**, 221911 (2005); 10.1063/1.1940130

AIP Applied Physics Reviews
NEW Special Topic Sections
NOW ONLINE
Lithium Niobate Properties and Applications: Reviews of Emerging Trends
AIP Applied Physics Reviews

Reuse of AIP Publishing content is subject to the terms at: https://publishing.aip.org/authors/rights-and-permissions. Download to IP: 143.54.44.137 On: Thu, 05 May 2016 17:49:54

Metal transport and loss in ultrathin hafnium aluminate films on silicon studied by low, medium, and high energy ion beam analyses

L. Miotti,[a] C. Driemeier, and F. Tatsch
Instituto de Física, Universidade Federal do Rio Grande do Sul, CP 15051, Porto Alegre, Rio Grande do Sul 91501-970, Brazil

C. Radtke
Pós-Graduação em Microeletrônica, Universidade Federal do Rio Grande do Sul, Porto Alegre, Rio Grande do Sul 91501-970, Brazil

I. J. R. Baumvol
CCET, Universidade de Caxias do Sul, Rio Grande do Sul 95070-580, Brazil and Instituto de Fisica, Universidade do Rio Grande do Sul, CP 15051, Porto Alegre, Rio Grande do Sul 91501–970, Brazil

(Received 7 March 2006; accepted 18 May 2006; published online 6 July 2006)

Metal transport and loss induced by thermal annealing in ultrathin $HfAl_xO_y$ films deposited on Si by atomic layer deposition were investigated by ion beam analysis. It was observed that rapid thermal annealing at 1000 °C induces decomposition of the aluminate films leading to Hf and Al losses mainly into the gas phase. It was possible to avoid this undesired decomposition effect by performing a postdeposition nitridation in NH_3 at 850 °C prior to the rapid thermal annealing step. The role of nitridation is discussed in terms of the profiles of incorporated N, before and after rapid thermal annealing, as determined by narrow resonant nuclear reaction profiling. © *2006 American Institute of Physics*. [DOI: 10.1063/1.2219150]

The replacement of silicon oxide or oxynitride by an insulator bearing higher dielectric constant (high κ) as the gate dielectric in the next generations of metal-oxide-semiconductor field effect transistors (MOSFETs) is predicted by the Semiconductor Industry Roadmap.[1] The search for a suitable high-κ material started by considering certain amorphous single oxide films, such as Al, Zr, Hf, La, and Gd oxides, that were predicted,[2,3] based on equilibrium phase diagrams, to be thermodynamically stable in contact with Si.

Much attention was given to HfO_2 films on Si due to its high dielectric constant (25–30) and the good electrical properties. However, HfO_2 films on Si crystallize at low temperature (~600 °C), forming poor barriers to electron transport as well as to O_2 migration. These two instabilities are minimized in Al_2O_3 dielectric films on Si but, on the other hand, the dielectric constant (9) is not sufficiently high. Previous authors[5–9] have shown that by adjusting the stoichiometry of $HfAl_xO_y$ films on Si it is possible to obtain insulating layers with reasonable dielectric constants.[8] Their crystallization temperatures were seen to be in most cases substantially higher than that of HfO_2 (Ref. 8) and they constitute in addition good diffusion barriers to oxygen.[6,7] Notwithstanding these advantages, mixed oxides or nanolaminates may present other instabilities[10–13] when submitted to postdeposition thermal annealing, such as (i) inhomogeneities in film stoichiometry, (ii) layer mixing in nanolaminated films, and (iii) loss of metallic (Hf, Al) species. Such instabilities arise from thermally activated net transport of atomic species across the high-κ/Si structure in metastable mixed oxides (pseudobinary alloys) or nanolaminates. Thus, before being integrated as high-κ gate dielectric in Si-based device fabrication technology, it is necessary to understand and control these instability effects. In this letter we report on the investigation of metal transport and loss during thermal annealing of Hf–Al mixed oxide and HfO_2/Al_2O_3 nanolaminate films on Si deposited by atomic layer deposition (ALD).[14]

Before depositing the aluminate films, the Si(100) substrates were wet chemically cleaned and a 1.1 nm thick SiO_2 layer was thermally grown. $HfCl_4/H_2O$ (HO) and $Al(CH_3)_3/H_2O$ (AO) were used as ALD precursors of HfO_2 and Al_2O_3, respectively.[9] Mixed $(HfO_2)_x(Al_2O_3)_{1-x}$ films were deposited with 1:1 and 5:1 HO/AO cycle ratios resulting in Al-rich ($x \approx 1/2$) and Hf-rich ($x \approx 6/7$) films as determined by ion beam analysis described below.[9] For simplicity, the $(HfO_2)_x(Al_2O_3)_{1-x}/SiO_2/Si$ films are hereafter called HfAlO/Si structures. A nanolaminated film was also deposited by the following route: 46 HO+5 AO+46 HO cycles. The resulting structure was an approximately 6.6 nm thick HfO_2 film on Si with an Al_2O_3 embedded layer ($HfO_2/Al_2O_3/HfO_2/Si$) thinner than 1 nm.[9]

The HfAlO/Si structures were processed in the typical dopant-activation thermal annealing step, namely, rapid thermal annealing (RTA) at 1000 °C in vacuum or in O_2-containing atmospheres, for 10 s. Although activation anneals during device processing are performed with a gate electrode such as metal or poly-Si in place, RTA was performed here on samples without a gate electrode, in order to allow for probing the dielectric film surface with ion beam analysis. Some selected samples were thermally nitrided in 20 mbars of NH_3 at 850 °C for 30 min prior to the 1000 °C RTA step. Isotopically enriched atmospheres were used for both RTA in O_2 and nitridation. The O_2 atmosphere was enriched to 97% in the ^{18}O isotope while the NH_3 atmosphere was enriched to 10% in the ^{15}N isotope. The profiles of the ^{18}O and ^{15}N isotopes incorporated into the HfAlO/Si structures were determined with nanometric depth resolution by narrow resonant nuclear reaction profiling (NRP),[15] using the $^{18}O(p,\alpha)^{15}N$ and $^{15}N(p,\alpha\gamma)^{12}C$ nuclear reactions[15] around the resonances at 151 and 429 keV, respectively. Furthermore, NRP analysis using the narrow resonances at 404.9 and 414 keV of the $^{27}Al(p,\gamma)^{28}Si$ (Ref. 16) and $^{29}Si(p,\gamma)^{30}P$ (Ref. 15) nuclear reactions were also used to determine, re-

[a]Electronic mail: miotti@if.ufrgs.br

Reuse of AIP Publishing content is subject to the terms at: https://publishing.aip.org/authors/rights-and-permissions. Download to IP: 143.54.44.137 On: Thu, 05 May 2016 17:49:54

 © 2006 American Institute of Physics

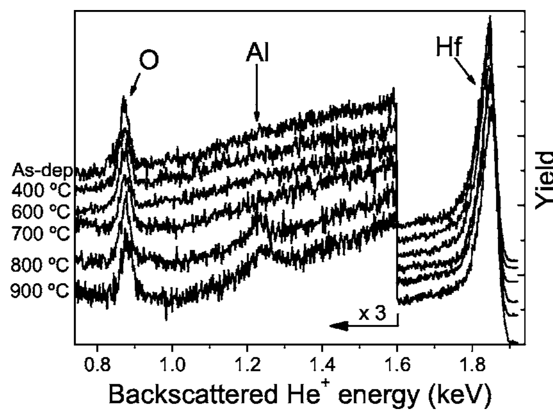

FIG. 1. (a) LEIS spectra of 2 keV He^+ ions detected at a scattering angle of 126° for a nanolaminated $(HfO_2/Al_2O_3/HfO_2)$ film on SiO_2/Si submitted to postdeposition annealing at the indicated temperatures.

spectively, the Al and Si profiles with nanometric depth resolution. Hafnium profiles were accessed by medium energy ion scattering (MEIS) of 100 keV H^+ ions. Hf areal densities were determined by Rutherford backscattering spectroscopy (RBS) of 1 MeV He^+ ions and Al areal densities by NRP using the resonance at 992 keV of the $^{27}Al(p,\gamma)^{28}Si$ nuclear reaction.[16] Low energy ion scattering[17] (LEIS) of 2 keV He^+ ions was used to investigate changes in the surface composition of the films induced by postdeposition annealing (PDA) in vacuum ($<10^{-6}$ mbar) for 30 min.

Aluminum transport was initially addressed by analyzing the surface composition of the nanolaminated stack $(HfO_2/Al_2O_3/HfO_2/Si)$ described above, as a function of PDA temperature in the 400–900 °C range. Figure 1 shows that only Hf and O contributed to the LEIS spectra of the as-deposited sample, as expected from a HfO_2 surface. No significant change is observed after annealing at temperatures up to 700 °C. However, a peak around 1.24 keV assigned to Al atoms on the film surface is present in the LEIS spectrum obtained after annealing at 800 °C, which increases slightly after annealing at 900 °C. Thus, annealing at and above 800 °C renders mobile Al atoms from the buried Al_2O_3 layer that can migrate to reach the sample surface and probably the interface as well.

Experimental and simulated excitation curves of the $^{27}Al(p,\gamma)^{28}Si$ nuclear reaction around the resonance at 404.9 keV are shown in Fig. 2(a), for an Al-rich (~5 nm) structure as deposited and for the same structure after RTA in 1 mbar of O_2. The corresponding Al profiles shown in the inset indicate Al loss from near-surface region as well as a reduction of the aluminate total areal density. Figure 2(b) shows the Hf regions of MEIS spectra obtained from a 6.5 nm thick Hf-rich structure, before and after RTA in the same conditions as above. The difference spectrum around proton energies of 95.5 keV shown in the inset reveals a reduction of the Hf concentration in the near-interface region, while the reduction of the energy width of the Hf signal after RTA confirms the reduction of the film thickness. The Hf and Al areal densities in the structures of Fig. 2 after RTA are given in Table I. Pronounced Al loss from the Al-rich structures and Hf loss from the Hf-rich structures are evident after RTA. Analysis of the near-interface regions of the Si substrate after RTA with back-secondary-ion-mass spectroscopy (not shown) revealed the migration of very small amounts of Hf and Al into this region. These results indicate

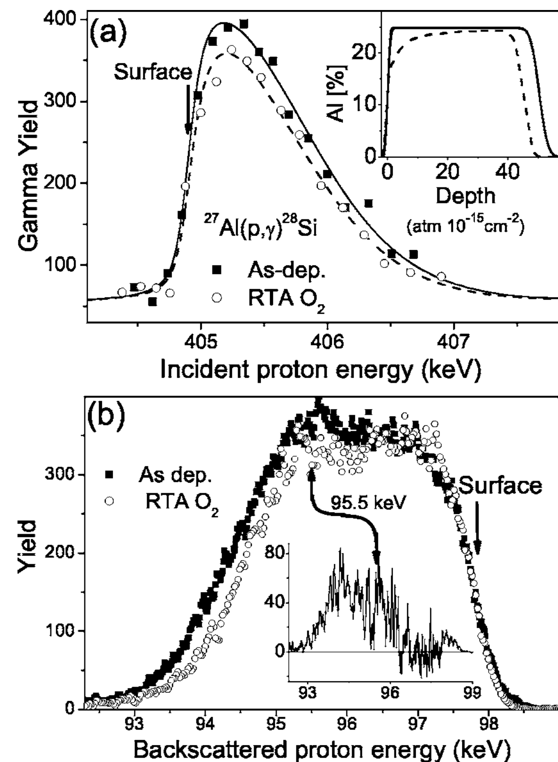

FIG. 2. (a) Excitation curves of the $^{27}Al(p,\gamma)^{28}Si$ nuclear reaction for an Al-rich structure on Si before and after RTA in 1 mbar of O_2. The Al profiles obtained simulating the excitation curves are shown in the inset. (b) Hf region of the MEIS spectra for a Hf-rich structure on Si before and after RTA in 1 mbar of O_2. The difference spectrum is shown in the inset.

that metal is lost by desorption during RTA of the HfAlO/Si structures.

Excitation curves of the $^{29}Si(p,\gamma)^{30}P$ nuclear reaction around the resonance at 414 keV for the same samples as in Fig. 2 are shown in Fig. 3. Comparing the low energy regions (around 414 keV) of the excitation curves, one notices that RTA did not promote Si migration into the aluminate neither exposure of the Si substrate. Only a small shift of the excitation curve for the Hf-rich structure toward higher energies is observed after RTA. This means that RTA promoted growth of a thin interfacial layer, most probably by oxidation of the Si substrate.[18]

TABLE I. Hf and Al areal densities in HfAlO/Si structures after RTA in the indicated atmosphere. Areal densities are normalized by their corresponding value in the as-deposited structure. Typical uncertainties are 3% and 15% for the normalized Hf and Al areal densities, respectively. The missing values were not measured or the annealing sequence was not performed.

		Non-nitrided		Nitrided	
Structure	RTA	Hf	Al	Hf	Al
Al rich ($x\approx 1/2$)	Vacuum	0.96	0.81	1.01	0.98
	0.1 mbar O_2	0.98	0.73	⋯	⋯
	1 mbar O_2	1.02	0.79	⋯	⋯
	10 mbar O_2	⋯	⋯	1.01	0.95
Hf rich ($x\approx 6/7$)	Vacuum	0.84	1.15	1.01	1.00
	0.1 mbar O_2	0.82	1.04	⋯	⋯
	1 mbar O_2	0.88	⋯	⋯	⋯
	10 mbar O_2	⋯	⋯	1.01	1.03

Reuse of AIP Publishing content is subject to the terms at: https://publishing.aip.org/authors/rights-and-permissions. Download to IP: 143.54.44.137 On: Thu, 05 May 2016 17:49:54

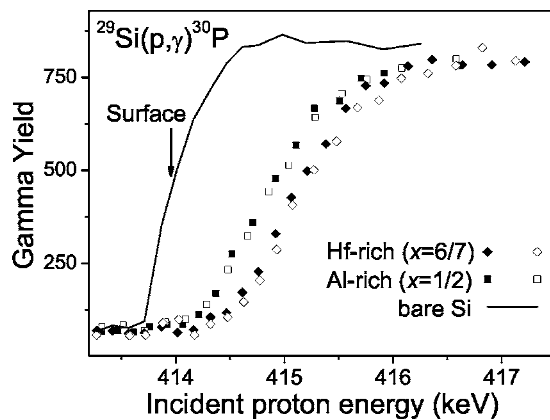

FIG. 3. Excitation curves of the $^{29}Si(p,\gamma)^{30}P$ nuclear reaction for the Hf- and Al-rich structures of Fig. 2 before (solid symbols) and after (empty symbols) RTA in 1 mbar of O_2. The excitation curve for a bare Si wafer is also shown to indicate the proton energy corresponding to ^{29}Si at the surface.

The normalized Hf and Al areal densities in 9 nm thick Hf-rich and 8 nm thick Al-rich films after nitridation and RTA at 1000 °C are also given in Table I. One notices from the data that thermal nitridation effectively suppressed both Hf and Al losses during RTA. The profiles in Fig. 4 show N incorporation mostly in near-surface and near-interface regions,[14] where a higher concentration of structural defects probably act as reactive sites for the observed N incorporation.[15] One can then associate the suppression of metal desorption with the reduction of atomic mobility in the HfAlO(N) films.[12] The ^{18}O profiles after RTA show, on the other hand, that most of the nitrogen lost during RTA was from near-surface regions, in exchange for oxygen from the gas phase. Thus, besides reducing the defect concentration, N is also sacrificially used to prevent Hf and Al transport near the surface. Nevertheless, the amount of ^{18}O incorporated in the nitrided HfAlO/Si structures were substantially lower than in previously reported non-nitrided HfAlO/Si structures.[18]

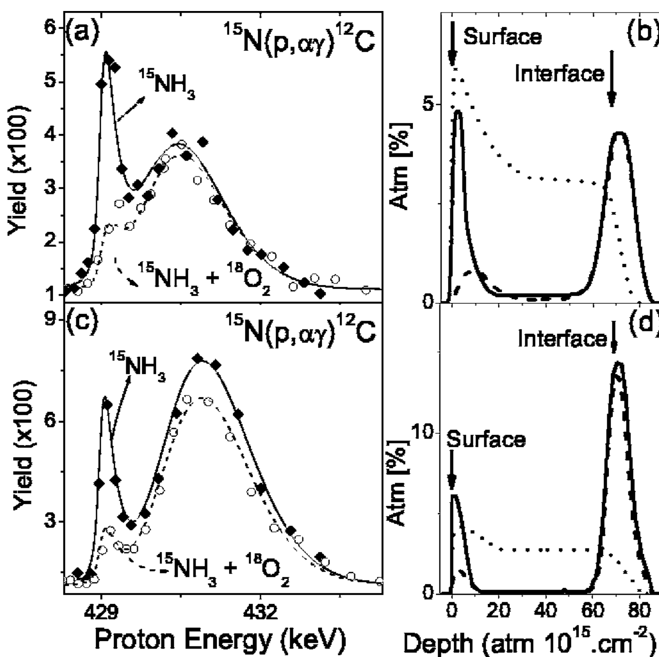

FIG. 4. Excitation curves of the $^{15}N(p,\alpha\gamma)^{12}C$ nuclear reaction for (a) nitrided Al-rich and (c) Hf-rich structures before (solid symbols, solid lines) and after (empty symbols, dashed lines) RTA in 10 mbars of $^{18}O_2$. (b) and (d) show the corresponding N profiles before (solid line) and after RTA (dashed line) obtained from simulation of the excitations curves. The N concentration was corrected using the 10% isotopic enrichment labeling of the NH_3 atmosphere used for nitridation. The ^{18}O profiles in the Al-rich (b) and Hf-rich (c) structures after the RTA in $^{18}O_2$ are also shown (dotted line). The vertical arrows indicate the areal density corresponding to the aluminate films and the surface.

Desorption of molecular species containing Hf and Al result from dissociation processes in the metastable Hf–Al oxide structures.[12,13] However, different from Hf(Zr) oxides and silicates this dissociation cannot be accounted by SiO desorption from the interfacial region as reported[19,20] by other authors. So, it is not likely that reactions at the dielectric/Si interface would play a significant role on the instabilities described here. Furthermore, in practical annealing situations, namely, with a gate electrode on top, desorption of Hf and Al would be prevented and these species would probably accumulate at the dielectric/electrode interface, reacting or not with the electrode material or, alternatively, migrating into the electrode film.

In summary, we studied the Hf and Al transport and loss in hafnium aluminate films on Si induced by postdeposition thermal processing. Hf and Al losses from the films indicate the decomposition of the films and desorption of both Hf- and Al-containing species. We also showed that it is possible to avoid this deleterious effect by nitriding the structures in a NH_3 atmosphere at a lower temperature prior to RTA.

The authors acknowledge the financial support provided by the Brazilian agencies CAPES, CNPq, and FAPERGS.

[1]The International Technology Roadmap for Semiconductors, Semiconductor Industry Association, 2004 Update; http://public.itrs.net/
[2]G. D. Wilk, R. M. Wallace, and. J. M. Anthony, J. Appl. Phys. **89**, 5243 (2001).
[3]K. J. Hubbard and D. G. Schlom, J. Mater. Res. **11**, 2757 (1996).
[4]M. Houssa, *High-k Dielectrics* (Institute of Physics Ltd., London, 2004).
[5]X. Y. Qiu, H. W. Liu, F. Fang, M. J. Ha, and J.-M. Liu, Appl. Phys. Lett. **88**, 072906 (2006).
[6]M. Park, J. Koo, J. Kim, H. Jeon, C. Bae, and C. Krug, Appl. Phys. Lett. **86**, 252110 (2005).
[7]M.-H. Cho, K. B. Chung, H. S. Chang, D. W. Moon, S. A. Park, Y. K. Kim, K. Jeong, C. N. Whang, D. W. Lee, D.-H. Ko, S. J. Doh, J. H. Lee, and N. I. Lee, Appl. Phys. Lett. **85**, 4115 (2004).
[8]M.-H. Cho, Y. S. Roh, C. N. Whang, K. Jeong, H. J. Choi, S. W. Nam, D.-H. Ko, J. H. Lee, N. I. Lee, and K. Fujihara, Appl. Phys. Lett. **81**, 1071 (2002).
[9]N. V. Nguyen, S. Sayan, I. J. R. Baumvol, C. Driemeier, C. Krug, L. Wielunski, and A. Diebold, J. Vac. Sci. Technol. A **23**, 1706 (2005).
[10]S. Monaghan, J. C. Greer, and S. D. Elliotta, J. Appl. Phys. **97**, 114911 (2005).
[11]Y. Yang, W. Zhu, T. P. Ma, and S. Stemmer, J. Appl. Phys. **95**, 3772 (2004).
[12]J. P. Chang and Y.-S. Lin, Appl. Phys. Lett. **79**, 3824 (2001).
[13]M.-H. Cho, H. S. Chang, Y. J. Cho, D. W. Moon, K.-H. Min, R. Sinclair, S. K. Kang, D.-H. Ko, J. H. Lee, J. H. Gu, and N. I. Lee, Appl. Phys. Lett. **84**, 571 (2004).
[14]M.-H. Cho, D. W. Moon, S. A. Park, Y. K. Kim, K. Jeong, S. K. Kang, D.-H. Ko, S. J. Doh, J. H. Lee, and N. I. Lee, Appl. Phys. Lett. **84**, 5243 (2005).
[15]I. J. R. Baumvol, Surf. Sci. Rep. **36**, 1 (1999) and references therein.
[16]R. P. Pezzi, M. Copel, C. Cabral, and I. J. R. Baumvol, Appl. Phys. Lett. **87**, 162902 (2005) and references therein.
[17]H. Niehus, W. Heiland, and E. Taglauer, Surf. Sci. Rep. **17**, 213 (1993).
[18]C. Driemeier, K. P. Bastos, L. Miotti, I. J. R. Baumvol, N. V. Nguyen, S. Sayan, and C. Krug, Appl. Phys. Lett. **86**, 472 (2005).
[19]S. J. Wang, P. C. Lim, A. C. H. Huan, C. L. Liu, J. W. Chai, S. Y. Chow, J. S. Pan, Q. Li, and C. K. Ong, Appl. Phys. Lett. **82**, 2047 (2003).
[20]S. Sayan, E. Garfunkel, T. Nishimura, W. H. Schulte, T. Gustafsson, and G. D. Wilk, J. Appl. Phys. **94**, 928 (2003).

Reuse of AIP Publishing content is subject to the terms at: https://publishing.aip.org/authors/rights-and-permissions. Download to IP: 143.54.44.137 On: Thu, 05 May 2016 17:49:54